



On a kinked crack model to describe the influence of material microstructure on fatigue crack growth

Andrea Spagnoli, Andrea Carpinteri, Sabrina Vantadori

Department of Civil-Environmental Engineering & Architecture (DICATEA), University of Parma

ABSTRACT. Threshold condition and rate of fatigue crack growth in both short and long crack regime appear to be significantly affected by the degree of crack deflection. In the present paper, a theoretical model of a periodically-kinked crack is presented to describe the influence of the degree of crack deflection on the fatigue behavior. The kinking of the crack is due to a periodic self-balanced microstress field having a length scale, d . By correlating the parameter d with a characteristic material length (e.g. average grain size in metals, maximum aggregate dimension in concrete), the possibility of using the present model to describe some experimental findings related to crack size effects in fatigue of materials is explored. Well-known experimental results concerning two different situations (fatigue threshold and fatigue crack growth in the Paris regime) are briefly analysed.

KEYWORDS. Kinked crack; Crack size effect; Fatigue crack growth; Fatigue threshold; Microstress field.

INTRODUCTION

Under fatigue loading, cracks in both brittle and ductile materials tend to deflect because of far-field multiaxial stresses, microstructural inhomogeneities (grain boundaries, interfaces, etc.), residual stresses, etc. Threshold condition and rate of fatigue crack growth in both short and long crack regime appear to be significantly affected by the degree of crack deflection [1]. This might be induced by the fact that the value of the near-tip Stress Intensity Factor (SIF) of kinked fatigue cracks can be considerably different from that of a straight crack of the same projected length.

In the case of bidimensional elastic problems, analytical solutions for SIF of kinked cracks are available in the literature [2-7]. Some of such results have been used to gain a quantitative understanding of the relation between fatigue crack growth rate and the degree of crack deflection in the fatigue crack path (e.g. see Ref. [8]).

A description of actual irregularities of kinked crack surfaces has been carried out by using the fractal geometry [9]. Successful applications of the fractal geometry to size effect-related fatigue problems have been proposed by the present authors in the past few years [10-16].

In this paper, a theoretical model of a periodically-kinked crack is discussed in order to describe the influence of the degree of deflection on the fatigue behavior. The kinking of the crack is due to a periodic self-balanced microstress field having a length scale, d [17]. By correlating the parameter d with a characteristic material length (e.g. average grain size in metals, maximum aggregate dimension in concrete), the possibility of using the present model to describe some experimental findings related to crack size effects in fatigue of materials is explored. Well-known experimental results concerning two different situations (fatigue threshold and fatigue crack growth in the Paris regime) are briefly analysed.

THE KINKED CRACK MODEL

Self-balanced microstress field

Consider an infinite cracked plate described by the xy coordinate system in Fig. 1, exposed to remote tensile stress $\sigma_y^{(\infty)}$ along the y -axis and shear stress $\tau_{xy}^{(\infty)}$. Assume that material microstructural features create a self-balanced (residual) microstress field, which is characterized by a length scale, d , related to a characteristic material length, and amplitudes e.g. governed by material properties' dispersion. Further let us assume that such a microstress field is a one-dimensional function (of the x - coordinate), defined by the following stress tensor:

$$\tilde{\mathbf{T}}(x) = \begin{bmatrix} \tilde{\sigma}_x & \tilde{\tau}_{xy} \\ \tilde{\tau}_{xy} & \tilde{\sigma}_y \end{bmatrix} = f\left(\frac{x}{d}\right) \begin{bmatrix} \tilde{\sigma}_{x,a} & \tilde{\tau}_{xy,a} \\ \tilde{\tau}_{xy,a} & \tilde{\sigma}_{y,a} \end{bmatrix} \quad (1)$$

Without lack of generality, we describe the plane microstress field by taking into account the following two non-zero stress components: $\tilde{\sigma}_y = \tilde{\sigma} = f(x/d)\tilde{\sigma}_a$ and $\tilde{\tau}_{xy} = \tilde{\tau} = f(x/d)\tilde{\tau}_a$. An attempt to correlate the above self-balanced microstress to some heterogeneity features of the material microstructure is presented in Ref. [18].

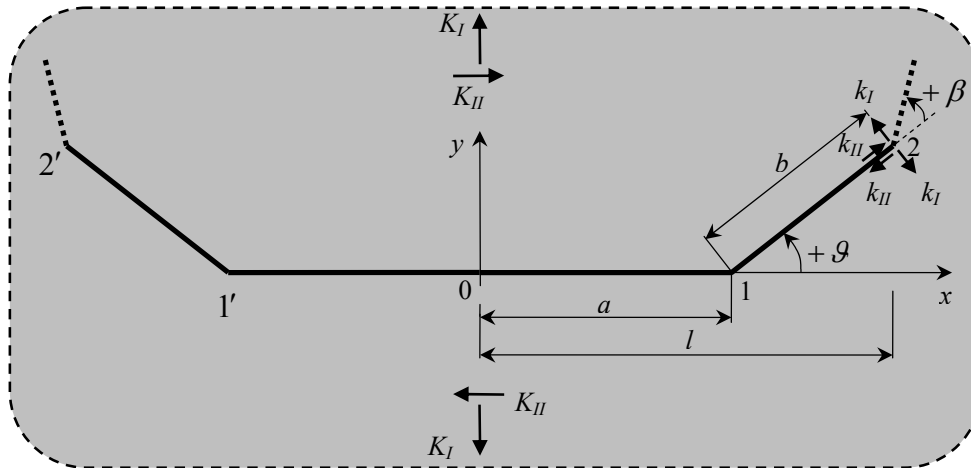


Figure 1: Nomenclature for the kinked crack in an infinite plate (y -axis of symmetry).

Approximate stress intensity factors in the kinked crack

According to the present model, the central crack might kink as a result of both remote and microstress fields (see Fig. 1). As will be shown below, the local stress intensity factors (SIFs) at the crack tips (k_I and k_{II}) can be expressed as a function of those (K_I and K_{II}) of a straight crack having length equal to the projected length of the kinked crack [2-7]. The total values of SIFs defined with respect to the projected crack are the sum of two contributions (due to remote and microstress fields, respectively), that is:

$$\begin{aligned} K_I &= K_I^{(\infty)} + \tilde{K}_I \\ K_{II} &= K_{II}^{(\infty)} + \tilde{K}_{II} \end{aligned} \quad (2)$$

The remote SIFs are defined with respect to the projected crack of semi-length l , aligned with the x - axis (Fig. 1). Hence, under the uniform remote stresses $\sigma_y^{(\infty)} = \sigma^{(\infty)}$ and $\tau_{xy}^{(\infty)} = \tau^{(\infty)}$, we have :

$$\begin{aligned} K_I^{(\infty)} &= 2\sigma^{(\infty)} \sqrt{\frac{1}{\pi}} \int_0^l \frac{1}{\sqrt{l^2 - x^2}} dx = \sigma^{(\infty)} \sqrt{\pi l} \\ K_{II}^{(\infty)} &= 2\tau^{(\infty)} \sqrt{\frac{1}{\pi}} \int_0^l \frac{1}{\sqrt{l^2 - x^2}} dx = \tau^{(\infty)} \sqrt{\pi l} \end{aligned} \quad (3)$$

The condition for self-balanced stress is that the function $f(x/d)$ is periodic (with material microstructure period d). For the sake of simplicity, we assume $f(x/d) = \cos(2\pi x/d)$ (this could be regarded as a first order approximation through Fourier series of a general periodic function). Now, since the above $f(x/d)$ is an even function with respect to x , we have that the value of the SIFs (i.e. referring to the projected crack) are (using Buckner's superposition principle, which is based on the stresses in the uncracked body along the crack lines):

$$\begin{aligned} \tilde{K}_I &= 2\sqrt{\frac{1}{\pi}} \int_0^1 \frac{\tilde{\sigma}}{\sqrt{1^2-x^2}} dx = 2\tilde{\sigma}_a \sqrt{\frac{1}{\pi}} \int_0^1 \frac{f(x/d)}{\sqrt{1^2-x^2}} dx = 2\tilde{\sigma}_a \sqrt{\frac{1}{\pi}} \int_0^1 \frac{\cos(2\pi x/d)}{\sqrt{1^2-x^2}} dx = \tilde{\sigma}_a \sqrt{\pi l} J_0\left(\frac{2\pi l}{d}\right) \\ \tilde{K}_{II} &= 2\sqrt{\frac{1}{\pi}} \int_0^1 \frac{\tilde{\tau}}{\sqrt{1^2-x^2}} dx = 2\tilde{\tau}_a \sqrt{\frac{1}{\pi}} \int_0^1 \frac{f(x/d)}{\sqrt{1^2-x^2}} dx = 2\tilde{\tau}_a \sqrt{\frac{1}{\pi}} \int_0^1 \frac{\cos(2\pi x/d)}{\sqrt{1^2-x^2}} dx = \tilde{\tau}_a \sqrt{\pi l} J_0\left(\frac{2\pi l}{d}\right) \end{aligned} \quad (4)$$

where J_0 is the zero order Bessel function.

In such a self-balanced microstress field, it can be reasonably assumed that the crack symmetrically kinks (due to the mixed mode of fracture) with respect to the y -axis and at each material microstructure semi-period, i.e. at each reversal in the microstress spatial courses ($a = d/2$ in Fig. 2). In the case of a singly-kinked crack (of projected crack length $2l$, as is reported in Fig. 1), the SIFs at the tips of the inclined part of the crack can be expressed through the SIFs K_I and K_{II} of a straight crack of length equal to the projected length of the kinked crack [2-7]:

$$\begin{aligned} k_I &= a_{11}(\vartheta, b/a) K_I + a_{12}(\vartheta, b/a) K_{II} \\ k_{II} &= a_{21}(\vartheta, b/a) K_I + a_{22}(\vartheta, b/a) K_{II} \end{aligned} \quad (5)$$

where a_{ij} are coefficients depending on the slant angle ϑ (positive counter-clockwise for tip coordinate $x > 0$) and the length ratio b/a between the deflected leading segment and the horizontal trailing segment. If a geometry different from that of an infinite plate with a central crack is examined, the geometric factor of the SIFs defined with respect to the projected crack would be different from the unity, but the expression in Eq. 5 would not change.

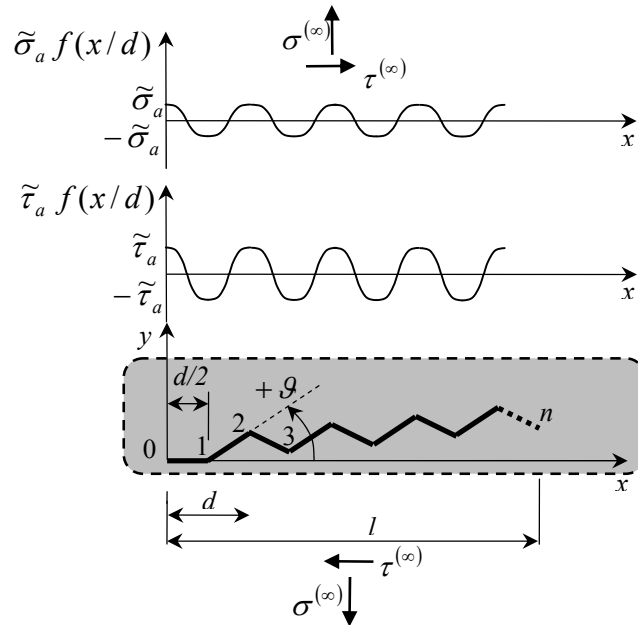


Figure 2: Mixed-mode crack growth in the self-balanced microstress field.

The coefficients a_{ij} for $b/a \rightarrow \infty$ (and, with good approximation, also for $b/a > 0.3$) are [2]:

$$\begin{aligned} a_{11}(\vartheta) &= \cos^{3/2} \vartheta & a_{12}(\vartheta) &= -2 \sin \vartheta \cos^{1/2} \vartheta \\ a_{21}(\vartheta) &= \sin \vartheta \cos^{1/2} \vartheta & a_{22}(\vartheta) &= \cos 2\vartheta \cos^{-1/2} \vartheta \end{aligned} \quad (6)$$



Note that the local SIFs in Eqs 5 and 6 are equal to those of an inclined straight crack of projected semi-length l forming an angle $\pi/2 - \mathcal{G}$ with respect to the loading axis of $\sigma^{(\infty)}$ [2].

It is reasonable to assume that, as the crack propagates following the path in Fig. 2, only its latter deflection influences the stress field near the crack tips (for example, the local SIFs at the crack tip 3 in Fig. 2 are assumed to be equal to those of a singly-kinked crack with an inclined segment corresponding to the segment 2-3, and by taking $b/a > 0.3$, see Eq. 6) [19]. The approximate computation is thus based on the assumption that the near-tip stress field depends on the local crack direction at the crack tip. The local SIFs at the crack tip are assumed to be expressed by Eqs 5 and 6 for deflected (Mode I+II) segments (see segments 1-2 and 1'-2' in Fig. 1), despite the fact that the length ratio b/a between the leading segment and preceding segment might in general vary from 0 to ∞ during propagation (in Fig. 1, for example, b is the running quantity for the crack propagating along the deflected segment 1-2 so that b/a ranges from 0 to a value greater than the unity).

Direction of growth of the kinked crack and effective SIF

As is mentioned above, the crack might kink at each material microstructure semi-period, namely at each reversal in the microstress spatial courses. The classical criterion of Erdogan and Sih [20] is applied herein to describe the mixed-mode crack propagation. Accordingly the kinking angle β , defined with respect to the general inclined axis of the crack (Fig. 1), is expressed by

$$\beta = 2 \arctan \left[\frac{1}{4} \frac{k_I}{k_{II}} \pm \frac{1}{4} \sqrt{\left(\frac{k_I}{k_{II}} \right)^2 + 8} \right] \quad (7)$$

where the SIFs values appearing in Eq. 7 are those determined according to Eqs 5 and 6. The angle β is positive counter-clockwise and is in the range $-\pi$ and $+\pi$. The sign in Eq. 7 is chosen so as to have the smallest absolute value of β .

Once the freshly formed kinked segment develops to a finite length, an equivalent SIF k_{eq} can be calculated according to Eqs 5 and 6. An effective driving force can be determined by applying the coplanar strain energy release rate theory [21], that is, the equivalent SIF k_{eq} is given by

$$k_{eq} = \sqrt{k_I^2 + k_{II}^2} \quad (8)$$

FATIGUE GROWTH IN NOMINALLY MODE I KINKED CRACKS

Now let us restrict our attention to nominally Mode I cracks, i.e. cracks submitted to a remote Mode I fatigue loading $\Delta\sigma^{(\infty)}$. Hence, for an infinite plate, we have the following SIFs related to the projected crack of semi-length l :

$$\begin{aligned} \Delta K_I &= \Delta\sigma^{(\infty)} \sqrt{\pi l} \left[1 + \frac{\Delta\tilde{\sigma}_a}{\Delta\sigma^{(\infty)}} J_0 \left(\frac{2\pi l}{d} \right) \right] = \Delta K_I^{(\infty)} \left[1 + \frac{\Delta\tilde{\sigma}_a}{\Delta\sigma^{(\infty)}} J_0 \left(\frac{2\pi l}{d} \right) \right] \\ \Delta K_{II} &= \Delta\sigma^{(\infty)} \sqrt{\pi l} \left[\frac{\Delta\tilde{\sigma}_a}{\Delta\sigma^{(\infty)}} J_0 \left(\frac{2\pi l}{d} \right) \right] = \Delta K_I^{(\infty)} \left[\frac{\Delta\tilde{\sigma}_a}{\Delta\sigma^{(\infty)}} J_0 \left(\frac{2\pi l}{d} \right) \right] \end{aligned} \quad (9)$$

In Eq. 9, we assume that the microstress field (e.g. $\Delta\tilde{\sigma}_a = \max_{t \in P} \tilde{\sigma}_a(t) - \min_{t \in P} \tilde{\sigma}_a(t)$) is time-varying and proportional to the applied remote loading of period P (constant amplitude fatigue loading).

Under remote Mode I loading and a superimposed shear microstress field, cracks propagate 'on average' along the x -axis following a zig-zag pattern (the same pattern is followed also in the presence of superimposed normal microstress). In general, it turns out that the crack slanting angle decreases as the crack length increases with respect to the material microstructural length d , namely $\mathcal{G} = \mathcal{G}(l/d)$.

Obviously, crack kinking occurs only in the presence of a multiaxial stress field. Therefore, for the simplest case of uniaxial remote and microstress fields, a coplanar growth of cracks occurs ($\mathcal{G} = 0$) and, according to Eq. 8, $\Delta k_{eq} = \Delta K_I$

with ΔK_I obtained from Eq. 9 (which includes the effect of the Bessel function J_0). No crack kinking occurs in such a case, but SIFs are not proportional to the square root of the crack length. Consequently, it can be shown that, in the bilogarithmic $dl/dN - \Delta K_I$ plane, crack growth does not follow a linear relationship (e.g. see Barenblatt's model to describe short fatigue crack growth in Ref. [19]).

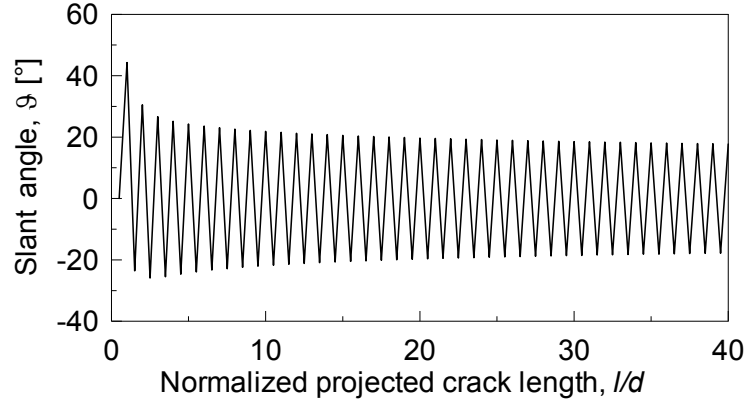


Figure 3: Example of slant angle variation under nominally Mode I loading ($d =$ characteristic material length).

Weighted average of effective stress intensity factor

A weighted average value $\Delta \bar{k}_{eq}$ of the equivalent SIF range Δk_{eq} along the straight segments is introduced. Recognizing a repetitive pattern constituted by n segments in the crack profile, we have :

$$\Delta \bar{k}_{eq} = \frac{\sum_{i=1}^n (s_i - s_{i-1}) \Delta k_{eq,i}}{s_n} \quad (10)$$

where $\Delta k_{eq,i}$ (see Eq. 8) is the equivalent SIF value along the straight segment of length $(s_i - s_{i-1})$, s being the curvilinear coordinate along the crack path (Fig. 4).

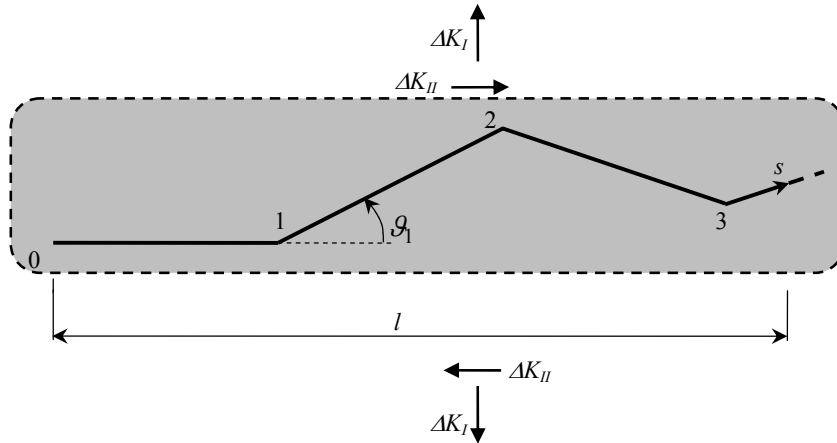


Figure 4: Fatigue growth of the kinked crack.

If the repetitive pattern is that of a zig-zag crack (this has been demonstrated to occur for remote/nominal Mode I load superimposed to any normal/shear microstress field), we have :

$$\Delta \bar{k}_{eq} = \frac{\frac{d}{2} \sum_{i=1}^n \frac{\Delta k_{eq,i}}{\cos \theta_i}}{\frac{d}{2} \sum_{i=1}^n \frac{1}{\cos \theta_i}} = \Delta K_I^{(\infty)} f(\theta, l/d, \Delta \tilde{\sigma}_a / \Delta \sigma^{(\infty)}, \Delta \tilde{\tau}_a / \Delta \sigma^{(\infty)}) \quad (11)$$



where the function $f = f(\mathcal{G}, l/d, \Delta\tilde{\sigma}_a/\Delta\sigma^{(\infty)}, \Delta\tilde{\tau}_a/\Delta\sigma^{(\infty)})$ highlights the dependence of $\Delta\bar{k}_{eq}$ on the relevant parameters. Note that the kinking angle is itself a function of l/d .

Geometric effects of kinking on crack growth rate

Considering the fact that, when the kinked crack spans a distance s , then the projected straight crack spans a distance l , the following relationship holds (between the crack growth rate, ds/dN , for the kinked crack and the nominal crack growth rate, dl/dN , for the projected straight crack) :

$$\frac{ds}{dN} = \frac{s}{l} \frac{dl}{dN} \quad (12)$$

Note that the crack rate dl/dN is always smaller than ds/dN . Now, for a zig-zag crack with slant angle \mathcal{G} , we have :

$$\frac{ds}{dN} = \frac{\frac{d}{2} \sum_{i=1}^n \frac{1}{\cos \mathcal{G}_i}}{\frac{d}{2} \frac{n}{dN}} \frac{dl}{dN} \quad (13)$$

Kinetics of fatigue crack growth

Now let us apply the Paris law to the periodically-kinked crack :

$$\frac{ds}{dN} = C \Delta\bar{k}_{eq}^m \quad (14)$$

where C and m are material constants.

By substituting Eqs 11 and 13 in Eq. 14, the following fatigue crack growth law in terms of the nominal quantities dl/dN and ΔK_I is determined for a zig-zag kinked crack :

$$\frac{dl}{dN} = C \frac{n}{\sum_{i=1}^n \frac{1}{\cos \mathcal{G}_i}} \Delta\bar{k}_{eq}^m \quad (15)$$

and hence, by using Eq. 11, we get :

$$\frac{dl}{dN} = C \frac{n}{\sum_{i=1}^n \frac{1}{\cos \mathcal{G}_i}} \left(\frac{\sum_{i=1}^n \Delta k_{eq,i}}{\sum_{i=1}^n \cos \mathcal{G}_i} \right)^m = C \left[f(\mathcal{G}, l/d, \Delta\tilde{\sigma}_a/\Delta\sigma^{(\infty)}, \Delta\tilde{\tau}_a/\Delta\sigma^{(\infty)}) \right]^m \left[\Delta K_I^{(\infty)} \right]^m \quad (16)$$

TWO APPLICATIONS OF THE KINKED CRACK MODEL TO EXPERIMENTAL EVIDENCES

For illustrative purposes, the present model is applied to some fatigue experimental evidences demonstrating crack size effects. The aim is to discuss whether the present model is able to follow some trend of behavior observed in the experimental tests. The comparison is carried out by considering, in the theoretical model, nominally Mode I cracks (the acting remote fatigue load is $\Delta\sigma^{(\infty)}$) under a shear microstress field with $\Delta\tilde{\tau}_a/\Delta\sigma^{(\infty)}$ arbitrarily taken to be equal to 2.

The first experimental data being analysed concern the fatigue threshold condition for mild steel [22]. Such data are related to ferritic and pearlitic steels with carbon content of 0.20% and grain size d of the ferritic phase equal to 7.8 μm (small-size grain) and 55 μm (large-size grain), respectively (see Ref. [12] for details of experimental data elaboration). For various values of the crack length (ranging from 6 to 1383 μm), the threshold stress intensity factor range ΔK_{th} was

experimentally evaluated (the threshold stress intensity $\Delta K_{th,0}$ for long cracks is equal to $5.21 \text{ MPa}\sqrt{\text{m}}$ and $6.20 \text{ MPa}\sqrt{\text{m}}$ for small-size grain and large-size grain material, respectively). Figure 5a reports, in a normalized form, the above experimental data along with the corresponding theoretical curve of the kinked model. Such a curve (normalized in so that the ratio $\Delta K_{th}/\Delta K_{th,0}$ tends to the unity for $l/d \rightarrow \infty$) is determined by posing the weighted average effective SIF of Eq. 11 equal to the threshold SIF range for long cracks $\Delta K_{th,0}$ (the remote SIF $\Delta K_1^{(\infty)}$ corresponds to the threshold SIF range ΔK_{th}), that is :

$$\frac{\Delta K_{th}}{\Delta K_{th,0}} = \frac{1}{f(\vartheta, l/d, \Delta \tilde{\tau}_a / \Delta \sigma^{(\infty)})} \tag{17}$$

It can be seen that the experimentally observed reduction of the threshold stress intensity factor with respect to that of long cracks (reduction occurring as the crack length decreases) is correctly captured by the present model, although to a smaller extent.

Further experimental data being analysed concern fatigue crack growth in the Paris regime [23, 24]. Such data are related to fatigue crack propagation in three-point bend specimens made of normal-strength (NS) plain-concrete [23] and high-strength (HS) plain-concrete [24]. For each concrete type, three series of two-dimensional geometrically similar cracked specimens with height b equal to 38, 76, 152mm and to 38, 108, 304mm for NS and HS concrete, respectively, span = $2.5b$, initial crack length $l_0 = 0.16b$, thickness = 38 mm. By elaborating the experimental data through a best-fit procedure (see Ref. [13] for details), it is shown that the Paris parameter m is independent of the initial crack length (m is equal to 10.4 and 8.2 for NS and HS concrete, respectively), while the Paris parameter C turns out to be dependent on such a length. Figure 5b plots the experimental best-fit values of C (for crack growth rate expressed in m/cycle and stress intensity range in $\text{MPa}\sqrt{\text{m}}$) as a function of the normalized initial crack length (the characteristic material length is taken to be equal to the maximum aggregate dimension, 12.7 and 9.5mm for NS and HS concrete, respectively), along with the best-fit curves of the present model (see Eq. 16, where the crack-size dependent Paris coefficient is $C \left[f(\vartheta, l/d, \Delta \tilde{\sigma}_a / \Delta \sigma^{(\infty)}, \Delta \tilde{\tau}_a / \Delta \sigma^{(\infty)}) \right]^m$). The experimental evidence seems to be well described by the present kinked model in the range of crack sizes being considered.

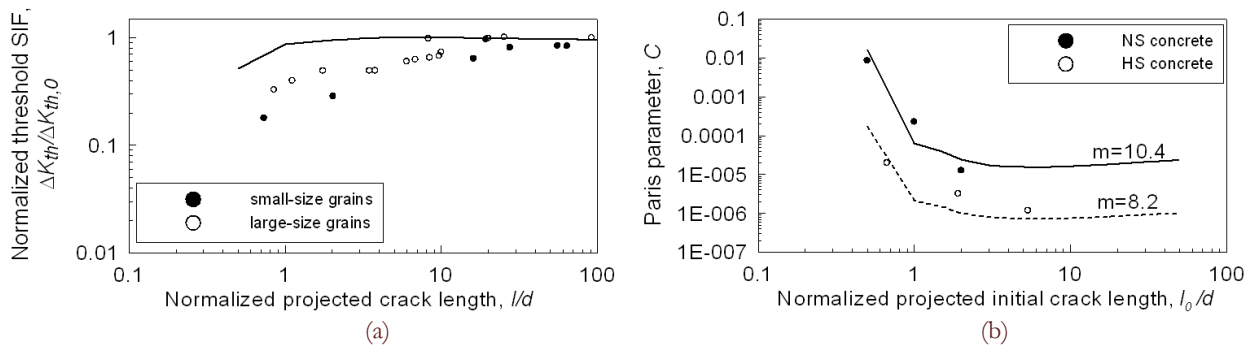


Figure 5: (a) Fatigue threshold results for mild steel [22]; (b) fatigue crack growth results in the Paris regime for concrete [23, 24].

CONCLUSIONS

In the present paper, irregular morphology of fracture surfaces is described via a two-dimensional model of a periodically-kinked crack, where its kinking is due to a periodic self-balanced microstress field having a length scale, d . On the basis of some geometrical and mechanical arguments, the model allows us to quantify the influence of the deflection degree on the fatigue threshold condition and fatigue crack growth. By correlating the parameter d with a characteristic material length (e.g. average grain size in metals, maximum aggregate dimension in concrete), the possibility of using the present model to describe some experimental findings related to crack size effects in fatigue of materials is explored. Some experimental results related to crack-size effects in fatigue threshold condition for metals as well as



fatigue crack growth in the Paris regime for concrete seem to be in favour of the present model, in the range of the crack sizes being considered.

ACKNOWLEDGEMENTS

The authors gratefully acknowledge the financial support of the Italian Ministry of Education, University and Research (MIUR) under the project PRIN 2009 No. 2009Z55NWC_003.

REFERENCES

- [1] Suresh, S., *Fatigue of materials*, 2nd edition, Cambridge University Press, Cambridge, (1998).
- [2] Kitagawa, H., Yuuki, R., Ohira, T., Crack-morphological aspects in fracture mechanics, *Engng Fract. Mech.* 7, (1975) 515-529.
- [3] Bilby, B.A., Cardew, G.E., Howard, I.C., Stress intensity factors at the tips of kinked and forked cracks, In: D.M.R. Taplin (Ed), *Fracture 3*, Pergamon Press, New York, (1977) 197-200.
- [4] Lo, K.K., Analysis of branched cracks, *J. App. Mech.*, 45 (1978) 797-802.
- [5] Cotterell, B., Rice, J.R., Slightly curved or kinked cracks, *Int. J. Fract.*, 16 (1980) 155-169.
- [6] Suresh, S., Shih, C.F., Plastic near-tip fields for branched cracks, *Int. J. Fract.*, 30 (1986) 237-259.
- [7] Chen, Y.Z., Stress intensity factors for curved and kinked cracks in plane extension, *Theor. and Appl. Fract. Mech.*, 31 (1999) 223-232.
- [8] Suresh, S., Crack deflection: implications for the growth of long and short fatigue cracks, *Metallurgical Transactions*, 14A (1983) 2375-2385.
- [9] Carpinteri, An., Scaling laws and renormalization groups for strength and toughness of disordered materials, *Int. J. Sol. and Struct.*, 31 (1994) 291-302.
- [10] Carpinteri, An., Spagnoli A., Vantadori, S., An approach to size effect in fatigue of metals using fractal theories, *Fat. & Fract. Engng Mat. & Struct.*, 25 (2002) 619-627.
- [11] Carpinteri, An., Spagnoli A., A fractal analysis of size effect on fatigue crack growth, *Int. J. Fat.*, 26 (2004) 125-133.
- [12] Spagnoli, A., Fractality in the threshold condition of fatigue crack growth: an interpretation of the Kitagawa diagram, *Chaos, Sol. and Fract.*, 22 (2004) 589-598.
- [13] Spagnoli, A., Self-similarity and fractals in the Paris range of fatigue crack growth, *Mech. Mat.*, 37 (2005) 519-529.
- [14] Carpinteri, An., Spagnoli, A., Vantadori, S., Viappiani, D., Influence of the crack morphology on the fatigue crack growth rate: a continuously-kinked crack model based on fractals, *Engng Fract. Mech.*, 75 (2008) 579-589.
- [15] Carpinteri An., Spagnoli A., Vantadori S., Size effect in S-N curves: a fractal approach to finite-life fatigue strength, *Int. J. Fat.*, 31 (2009) 927-933.
- [16] Carpinteri, An., Spagnoli, A., Vantadori, S., A multifractal analysis of fatigue crack growth and its application to concrete, *Engng Fract. Mech.*, 77 (2010) 974-984.
- [17] Carpinteri, An., Spagnoli, A., Vantadori, S., Correlating the fractal dimension of a continuously-kinked fatigue crack with some material microstructural features, In: *Proceedings of The 13th International Congress on Mesomechanics* Vicenza, Italy, (2011).
- [18] Barenblatt, G. I., On a model of small fatigue cracks, *Engng Fract. Mech.*, 28 (1987) 623-626.
- [19] Brighenti, R., Carpinteri, A., Spagnoli, A., Scorza, D., Crack path dependence on inhomogeneities of material microstructure, *Frattura ed Integrità Strutturale*, 20 (2012) 6-16.
- [20] Erdogan, F., Sih, G.C., On the crack extension in plates under plane loading and transverse shear, *J. Basic Engng.*, 85 (1963) 519-527.
- [21] Sih, G.C., Strain-energy-density factor applied to mixed mode crack problems, *Int. J. Fract.*, 10 (1974) 305-321.
- [22] Tanaka, K., Nakai, Y., Yamashita, M., Fatigue growth threshold of small cracks, *Int. J. Fat.*, 17 (1981) 519-33.
- [23] Bazant, Z.P., Xu, K., Size effect in fatigue fracture of concrete, *ACI Mat. J.*, 88 (1991) 390-399.
- [24] Bazant, Z.P., Shell, W.F., Fatigue fracture of high-strength concrete and size effect, *ACI Mat. J.*, 90 (1993) 472-478.